The impact of water erosion on global maize and wheat productivity

Tony W. Carr[1]*, Juraj Balkovič[2,3], Paul E. Dodds[1], Christian Folberth[2] and Rastislav Skalský[2,4]

[1]University College London, Institute for Sustainable Resources, London, United Kingdom

[2] International Institute for Applied Systems Analysis, Ecosystem Services and Management Program, Laxenburg, Austria

[3] Comenius University, Faculty of Natural Science, Bratislava, Slovakia

[4] National Agricultural and Food Centre, Soil Science and Conservation Research Institute, Bratislava, Slovakia

* Correspondence to: Tony Carr (tony.carr.16@ucl.ac.uk)

Abstract

Water erosion removes soil nutrients, soil carbon, and in extreme cases can remove topsoil altogether. Previous studies have quantified crop yield losses from water erosion using a range of methods, applied mostly to single plots or fields, and cannot be systematically compared. This study assesses the worldwide impact of water erosion on maize and wheat production using a global gridded modelling approach for the first time. The EPIC crop model is used to simulate the global impact of water erosion on maize and wheat yields, from 1980 to 2010, for a range of field management strategies. Maize and wheat yields were reduced by a median of 3% annually in grid cells affected by water erosion, which represent approximately half of global maize and wheat cultivation areas. Water erosion reduces the annual global production of maize and wheat by 8.9 million tonnes and 5.6 million tonnes, with a value of $3.3bn globally. Nitrogen fertilizer necessary to reduce losses is valued at $0.9bn. As cropland

most affected by water erosion is outside major maize and wheat production regions, the production losses account for less than 1% of the annual global production by volume. Countries with heavy rainfall, hilly agricultural regions and low fertilizer use are most vulnerable to water erosion. These characteristics are most common in South and Southeast Asia, sub-Saharan Africa and South and Central America. Notable uncertainties remain around large-scale water erosion estimates that will need to be addressed by better integration of models and observations. Yet, an integrated bio-physical modelling framework - considering plant growth, soil processes and input requirements - as presented herein can provide a link between robust water erosion estimates, economics and policy-making so far lacking in global agricultural assessments.

1. Introduction

Soil erosion through rainfall and water runoff, washes away topsoil and degrades soil structure, which can reduce crop yields. Water erosion affects a variety of soil functions relevant for crop growth such as nutrient levels, pH, water-holding capacity, texture, infiltration rates and soil organic matter (den Biggelaar et al., 2001). The main factors determining the degree of water erosion are precipitation strength, slope steepness, soil structure and vegetation cover. Apart from precipitation, the primary factors influencing water erosion can be directly altered through field management such as the choice of crops, reducing tillage intensity, fallow and crop residue cover, and terracing and contour ploughing (Panagos et al., 2016; Poesen, 2018).

Productivity loss through water erosion and other processes, such as the depletion of soil nutrients, is defined as land degradation (Vogt et al., 2011). Although no clear consensus on the global extent of land degradation exists, it has become clear that a considerable amount

of cropland is degraded and threatened by productivity loss. In a review of most prominent land degradation assessments, Gibbs and Salmon (2015) estimated that 1–6 billion ha of ice-free land surface (up to 66%) is degraded to varying degrees. Most studies agree that water erosion is one of the most serious land degradation processes, especially in developing countries (FAO and ITPS, 2015; Montanarella et al., 2016; Oldeman et al., 1991). Furthermore, several studies point out that land degradation disproportionately affects populations under social and economic pressures, who are more exposed to degraded land and are often forced to have an unsustainable reliance on available resources (Nachtergaele et al., 2011; Wynants et al., 2019). The negative effects of land degradation on social and economic well-being has been widely recognised. Yet its present and future impacts are not adequately quantified globally in physical and economic terms to inform major environmental and agricultural policies (Montanarella, 2007; Montanarella et al., 2016; Nkonya et al., 2011).

Soil loss due to water erosion has been estimated at many sites worldwide and modelled globally (Borrelli et al., 2017; Doetterl et al., 2012; García-Ruiz et al., 2015; Montgomery, 2007). However, from a food security standpoint, it is more relevant to quantify the impact of water erosion on crop productivity. There are substantial variations in the estimates of productivity losses from the few studies in the literature (Bakker et al., 2004, 2007; Den Biggelaar et al., 2004b; van den Born et al., 2000; De la Rosa et al., 2000; Lal, 1995; Larney et al., 2009; Oyedele and Aina, 1998). This variability is not surprising as erosion-productivity relationships are difficult to generalize due to the location-specific nature of soil erosion determined by soil properties, climate and management (Den Biggelaar et al., 2004a). Moreover, the choice of method to measure water erosion impacts on crops is one of the most important factors explaining variations between studies (Bakker et al., 2004). Hence, different methodological approaches in field studies can mask the impact of regional differences on water erosion impacts on crops.

Previous global erosion impact assessments (Pimentel et al., 1995; Sartori et al., 2019) relied on simple linear assumptions about the impact of water erosion on crop yields, and neglected

differences between crops and regional characteristics. Crop models can facilitate the extrapolation of experimental and small-scale data across a range of environments and management strategies (Nelson et al., 1996). Moreover, models are essential to determine long-term effects of degradation processes, which are challenging to observe in short-term field experiments (Enters, 1998). Crop models combined with global gridded data infrastructure are increasingly used for climate change impact assessments, evaluations of agricultural externalities, and as input data providers for agro-economic models (Elliott et al., 2014; Mueller et al., 2017; Nelson et al., 2014). However, most of the global gridded crop modelling (GGCM) studies have so far neglected soil erosion and its impact on crop yield and production.

In this study, we use a GGCM platform to quantify global potential crop productivity losses due to water erosion for the first time. We examine maize and wheat as representative staple crops, due to their wide distribution in global agriculture and their contrasting soil cover patterns. We assess the overall impact of water erosion on global maize and wheat production, for a variety of field management techniques, and identify the most vulnerable regions based on environmental conditions and fertilizer use. Finally, we consider the uncertainties in our assessment.

2. Methods

We use the gridded crop model EPIC-IIASA (Balkovič et al., 2014), which combines the biophysical Environmental Policy Integrate Climate (EPIC) model with global data on soil, climate and crop management, to simulate the daily growth of maize and wheat with and without the impact of water erosion on a global scale. This approach enables us to assess, based on a globally consistent method, the impact of water erosion on maize and wheat productivity relative to a reference scenario where water erosion is excluded from simulations and has no impact on crop growth. In both cases, the simulations account for a variety of environmental drivers, farming techniques and farm inputs such as fertilizers and irrigation.

Importantly, this approach enables us to identify regions which are vulnerable to water erosion, and to quantify a production volume that is under threat due to water erosion. Our simulation results reflect long-term impacts of water erosion following continuous cultivation for 31 years, based on daily weather data for the period 1980–2010. In addition, we use a range of field management scenarios to address the highly influential impact of farming techniques on water erosion impact assessments, which are among the main sources of uncertainty at the global scale (Carr et al., 2020).

1.1   The EPIC model

EPIC can simulate a wide range of crops and relevant soil and hydrological processes controlling carbon, nutrient and water dynamics (Izaurralde et al., 2006). The relevant model processes to simulate crop growth and water erosion presented in the following are based on their description in the EPIC model documentation (Sharpley and Williams, 1990).

Phenological development of a crop is based on the heat unit (HU) approach. This involves a base temperature providing a crop-specific threshold under which no growth occurs, and the sum of daily HUs (°C) accumulated during crop growth stages needed to determine when a crop reaches maturity. In our study, the potential HUs determining crop maturity are based on long-term climate data and reported growing seasons provided for different global environments by Sacks et al. (2010). Daily potential biomass growth is determined by intercepted photosynthetically active radiation based on the leaf area index (LAI) and solar radiation. The LAI of wheat and maize increases exponentially during early vegetative growth, after a plateauing it reaches a maximum at maturity, and continuously decreases afterwards. A dormancy period is considered in case of autumn-sown wheat cultivars. LAI is calculated as a function of heat units, crop stress, and crop development stages. Total biomass is split between above- and below-ground biomass. At maturity, crop yield is calculated by multiplying the total above-ground biomass with a harvest index, which is affected by heat units. Potential crop growth and crop yields are constraint mainly by water, nutrients (N and P), temperature

and aeration stress. The most severe stress factor on a given day limits biomass accumulation, root growth and yield by a fraction ranging from 0 to 1.

EPIC includes seven empirical equations to calculate water erosion (Wischmeier and Smith, 1978). The basic equation is:

$$E = R * K * LS * C * P \quad (1)$$

where E is soil erosion in t ha^{-1} (mass/area), R is the erosivity factor (erosivity unit/area), K is the soil erodibility factor in t MJ^{-1} (mass/erosivity unit), LS is the slope length and steepness factor (dimensionless), C is the soil cover and management factor (dimensionless) and P is the conservation practices factor (dimensionless). In this study, we use the MUSS equation (Williams, 1995), which is adapted for small watersheds:

$$R = 0.79 * (Q * q_p)^{0.65} * WSA^{0.009} \quad (2)$$

where Q is runoff volume (mm), q_p is peak runoff rate (mm h^{-1}) and WSA is watershed area (ha). In a comparison of the seven water erosion equations included in EPIC, simulated water erosion values based on the MUSS equation match closest with observed water erosion rates from 606 measurements on arable land around the world (Carr et al., 2020) (For a summary of the comparison of simulated erosion rates with field measurements, see Text S1.). In EPIC, the main impact of water erosion on crops is driven by nutrient stress through the export of organic carbon, nitrogen and phosphorus from the topsoil layer through sediment runoff. The soil organic matter model in EPIC is based on the Century model (Izaurralde et al., 2006). The system interacts directly with soil moisture, temperature, erosion, tillage, soil density, soil texture, leaching, and translocation functions.

1.2 Global gridded EPIC model

The EPIC-IIASA GGCM has 131,326 grid cells with a resolution varying between 5' x 5' and 30' x 30' (approximately 9 km and 56 km, respectively, at the equator). The smallest spatial elements of the grid cells are global datasets of soil and topography with a resolution of 5' x 5'. Soil information includes soil type, texture, bulk density and organic carbon concentration

from the Harmonized World Soil Database (FAO/IIASA/ISRIC/ISSCAS/JRC, 2012), and topography data is taken from USGS GTOPO30 (USGS, 1997). Within a domain of 30' x 30' grids, the elements belonging to identical topography and soil texture classes, and falling within the same country, are spatially aggregated to grid cells. Each grid cell is represented by a single field characterized by the prevailing combination of topography and soil conditions found in the landscape. Slope length (20 – 200m) and field size (1 – 10ha) are allocated to each representative field based on a set of rules for different slope classes (Table S1). The slope of each representative field is determined by the slope class covering the largest area in each grid cell (Table S1). Slope classes are taken from a global terrain slope database (IIASA/FAO, 2012) and are based on a high-resolution 90 m SRTM digital elevation model. Weather data, including daily precipitation (mm), minimum and maximum temperatures (°C), solar radiation (MJ m^{-2}) and relative humidity (%), are used at a spatial resolution of 0.25° x 0.25°. We use historic bias-corrected daily weather data combining data from the MERRA reanalysis model, station data, and remotely sensed datasets, covering the years 1980–2010 (AgMERRA, Ruane et al., 2015). Rainfed and irrigated maize and wheat production areas for each grid cell are taken from Portmann et al. (2010) We base crop management on reported growing seasons (Sacks et al., 2010) and spatially explicit nitrogen and phosphorus fertilizer application rates (Mueller et al., 2012).

1.3 Field management scenarios

Maize and wheat have contrasting soil cover densities. Maize is typically cultivated in wide rows, which leaves the soil surface less protected than in wheat fields, where crops are grown in a higher density. We simulate each crop for six field management scenarios (three tillage x two cover crop scenarios), each influencing soil properties, water erosion and plant growth differently. In grid cells in which several of these scenarios coincide (see below), simulation results are subsequently averaged. The tillage management scenarios represent conventional, reduced and no-tillage, which differ by tillage depth, mixing efficiency of tillage and sowing mechanizations, surface roughness and the amount of plant residues left on the

field after crop harvest (Table 1). In addition, we alter the runoff curve numbers for each tillage scenario to account for different runoff intensities for the cover treatment classes presented in Table 1. Runoff curve numbers indicate the runoff potential of a hydrological soil group, land use and treatment class and allow to take the impact of different tillage practices on the hydrologic balance into account (Chung et al., 1999). The different tillage intensities account for the impact of gradually changing surface cover and roughness on water erosion rates. We simulate each tillage scenario with and without cover crop (grass-type green fallow) in between growing seasons.

The field management scenarios reflect a range of potential impacts occurring due to different farming techniques on erosion–crop yield relationships. To account for geographic variations in field management, we construct a baseline wheat and maize management scenario from the six alternatives based on the climatic and country-specific indicators as follows:

- As the only global statistical data on the type of tillage systems are provided for the extent of Conservation Agriculture area at the national scale (FAO, 2016), we assign only the lowest tillage intensity scenario to specific countries in our baseline scenario. Therefore, conventional and reduced tillage are simulated in each grid cell globally, whereas the additional no-tillage scenario is simulated only for countries in which at least 5% of cropland is cultivated under conservation agriculture according to AQUASTAT (2007–2014) (FAO, 2016), including Argentina, Australia, Bolivia, Brazil, Canada, Chile, China, Colombia, Finland, Italy, Kazakhstan, New Zealand, Paraguay, Spain, USA, Uruguay, Venezuela, Zambia, and Zimbabwe (Figure S7).

- The simulation of green fallow in between growing seasons is determined by the main Köppen-Geiger regions (Kottek et al., 2006). In tropical regions, we simulate cover crops in between maize and wheat seasons to represent soil cover from a year-round growing season. In arid regions, we do not simulate cover crops in between growing seasons due to limited water supply. In temperate and snow regions, we use average simulation results from both cover crop scenarios (Figure S7).

- Irrigation and conservation practices in all field management scenarios are based on the underlying slope class of each grid cell (Table S1). On slopes steeper than 5%, we consider only rainfed agriculture, as hilly cropland is irrigated predominantly on terraces that prevent water runoff.

- P-factors can be used to simulate conservation practices. These are static coefficients ranging between 0 and 1, where 0 represents conservation practices that prevent any erosion and 1 represents no conservation practices. Whilst we introduced conservation practices implicitly through various crop growth assumptions as presented in Table 1, we showed in a previous study (Carr et al., 2020) that P-factors (i.e., additional, or more efficient conservation practices) should be used on steep slopes to prevent EPIC from overestimating water erosion. As there is presently no globally consistent information on the distribution of conservation practices, we assigned P-factors <1 to slopes > 16% assuming that conservation practices are most likely implemented on steep slopes. On slopes steeper than 16%, we assign a P-factor of 0.5, and on slopes steeper than 30%, we assign a P-factor of 0.15 to simulate contouring and terracing based on the range of P-values presented in Morgan (2005).

To determine the impact of water erosion on maize and wheat yields, we simulate all field management scenarios additionally with no erosion (P=0). The comparison of crop yields simulated with a P-factor value of zero with crop yields simulated under higher P-factor values can be used to identify grid cells where crop yields are reduced by water erosion. We use the simulation outputs at those grid cells to quantify the reduction of maize and wheat production and the relative reduction of crop yields due to water erosion.

1.4 Uncertainties in the cultivated slope and field management data

Assumptions about land topography and field management have a significant impact on estimated water erosion rates. This is particularly important because global data on land use is uncertain and the use of different farming techniques are not well understood, and this could introduce errors into our analysis.

While we know the range of slopes and the fraction of cropland in each grid cell, we do not know how much land in each slope class is cultivated. We therefore assume the cropland in each grid cell is on the slope class that is most common in the grid cell, as this represents the prevailing topographical conditions. This assumption is likely to introduce spatially-varying uncertainty as the fraction of each grid cell containing the dominant slope category varies from 20% to 100%, with an average share of 48%. The share of land covered by cropland in each grid cell also varies greatly, from 1% to 100%, with an average share of 14% (Figure S6). Therefore, the extrapolation of our simulation outputs to the entire cultivated area in a grid cell can provide only a rough estimate of the global differences in maize and wheat production losses due to water erosion.

We explore the implications of this assumption by comparing our simulation results to a second set of simulation outputs based on an ideal cropland distribution scenario, in which the flattest terrain available rather than the most common slope in each grid cell is cultivated. This assumes that farmers would prefer to cultivate flatter land where possible. As this requires a large number of additional model runs for various combinations of slope assumptions and field management scenarios per grid cell, we use an example region to reduce computational time. We examine Italy, as it is susceptible to water erosion and includes large and heterogenous maize and wheat cultivation areas on flat terrain in the north and mountainous regions in the south.

We address field management uncertainties by examining the range between minimum and maximum water erosion impacts on crops simulated with all field management scenarios for each grid cell and country.

1.5 Crop yield and production impact aggregation

Simulated maize and wheat yields, which are calculated in t ha^{-1} dry matter, are converted to fresh matter assuming a net water content of 12% following Wirsenius (2000), so that they can be compared with yields reported by FAOSTAT (FAO, 2020). To determine the impact of

water erosion on maize and wheat yields by the end of the simulation period, we average crop yields generated with all relevant field management scenarios selected under the baseline scenario assumptions for the years 2001–2010. We weight mean crop yields by the irrigated and rainfed cultivation area (Portmann et al., 2010) of the respective crop per grid cell (Equation 3). The difference between average maize and wheat yields, simulated with and without the impact of water erosion, are used to filter grid cells where water erosion reduces crop yields (i.e. the area where crop yields are vulnerable to water erosion). Subsequently, the relative reduction of maize and wheat yield due to water erosion is calculated on grid cell level (Equation 4).

$$Yw_{cpg} = Yav(r)_{cpg} * Af(r)_{cg} + Yav(i)_{cpg} * Af(i)_{cg} \qquad (3)$$

$$dYrel_{cg} = \frac{Yw(e0)_{cg} - Yw(e1)_{cg}}{Yw(e0)_{cg}} \; ; if \; Yw(e0)_{cg} > Yw(e1)_{cg} \qquad (4)$$

Yw$_{cpg}$ is area-weighted mean crop fresh matter yield (t ha^{-1}) for crop *c*, P-factor value *p* and grid cell *g*; *Yav* is yield averaged across the tillage and cover crop scenarios selected in each grid following the baseline scenario assumptions and for the years 2001–2010 simulated under irrigated (i) and rainfed (r) conditions; *Af(r)* is the rainfed area fraction; and *Af(i)* is the irrigated area fraction. *dYrel* is the relative loss of the yield of crop *c*, at grid cell *g*; *Yw* is weighted average yield simulated with a P-factor value of 0 (e0) and a P-factor value greater than 0 (e1).

To calculate the loss of crop production in each country, we first estimate the absolute reduction of crop yields as the difference in the mean yield for the years 2001–2010 simulated without and with water erosion (e0 and e1, respectively) (Equation 5). We then multiply this yield reduction by the total area of irrigated and rainfed cropland of each grid cell in the country (Equation 6).

$$dYabs_{cwg} = Yav(e0)_{cwg} - Yav(e1)_{cwg}; if \; Yw(e0)_{cpg} > Yw(e1)_{cpg} \qquad (5)$$

$$dP_{lc} = \sum_{g=1}^{n} dYabs(i)_{cg} * A(i)_{cg} + dYabs(r)_{cg} * A(r)_{cg} \qquad (6)$$

dYabs$_{cwg}$ is the absolute yield loss for crop *c*, irrigation scenario *w* and grid cell *g; Yav* is yield averaged across the tillage and cover crop scenarios selected in each grid cell following the baseline scenario assumptions and for the years 2001–2010 with P=0 (e0) and a P>0 (e1); *dP$_{lc}$* is the loss of production (in tonnes) of crop *c* in country *l*; *n* is the number of grid cells in country *l*; *dYabs(i)* is the absolute decline in irrigated yields and *dYabs(r)* is the absolute decline in rainfed yields; *A(r)* is the rainfed area (in ha); and *A(i)* is the irrigated area (in ha).

We use the national market prices of crops from the FAOSTAT producer price (average 2013–2018, or the last five annual records available) to calculate the economic maize and wheat production losses (in $) due to water erosion per country and globally. Two-tailed T-tests are used to filter countries with significant differences between average yields simulated with and without water erosion.

1.6 Evaluation of the quality of the modelled crop yields

We evaluate modelled maize and wheat yields (Figure S5) against FAOSTAT reported yields using the baseline crop management scenario. We convert modelled dry-matter crop yields to fresh matter and aggregate yields for each country using the same approach as for grid cell-level aggregation in Equation 3. We average irrigated and rainfed crop yields (generated with all P-factor values, tillage and cover crop scenarios selected for the baseline scenario and the years 2001 and 2010) for each country and weight them by the cultivated area of the respective irrigated or rainfed crop per country (Portmann et al., 2010) (Equation 7). We use average maize and wheat yields per grid cell to summarise the total maize and wheat production for each country (Equation 8).

$$Yw_{cl} = Yav(r)_{cl} * Af(r)_{cl} + Yav(i)_{cl} * Af(i)_{cl} \qquad (7)$$

$$P_{cl} = \sum_{g=1}^{n} Yav(r)_{cg} * A(r)_{cg} + Yav(i)_{cg} * A(i)_{cg} \qquad (8)$$

Yw$_{cl}$ is weighted yield for crop *c* in country *l; Yav* is yield averaged for the years 2001–2010, with all P-factor values and all tillage and cover crop scenarios selected under the baseline scenario assumptions simulated under irrigated *(i)* and rainfed *(r)* conditions; *Af(r)* is the

rainfed area fraction and *Af(i)* is the irrigated area fraction; P_{cl} is the total production (in tonnes) of crop *c* in country *l*; *g* is any grid cell in country *l*; *n* is the number of grid cells in country *l*; *A(r)* is the rainfed area and *A(i)* is the irrigated area in hectares.

We compare crop yields and total production per country against FAOSTAT statistics for the years 1995–2005. The years are chosen based on the years of reported fertilizer application rates that are used to simulate maize and wheat yields. The agreement between simulated and reported data is determined by the coefficient of determination (R^2) and the relative error (%) between both datasets. Evaluation results are provided in the supplementary information (Text S2, Figure S3, Figure S4).

2   Results

2.1   The impact of water erosion on global maize and wheat yields

In the last decade of our 31-year simulation period, the average annual maize and wheat yields were reduced due to water erosion at 58% and 62% of grids cells, respectively, by a global median of 3% for each crop. The affected grid cells represent 51% and 46% of global maize and wheat cultivation areas, respectively. Median annual soil loss at grid cells where crop yields are reduced is 11 t ha^{-1} and 6 t ha^{-1} on maize and wheat fields, respectively. The simulated relative reduction of average annual maize and wheat yields per grid cell at the end of the simulation period is illustrated in Figure 1. Most grid cells where high yield reduction is simulated represent fields with low fertilizer input on steep slopes exposed to intensive precipitation.

The distribution of annual average crop yield losses for the 40 most vulnerable maize- and wheat-producing countries is plotted in Figure 2. Countries in which the median annual reduction of maize yields due to water erosion is higher than 5% by the end of the simulation period are most abundant in sub-Saharan Africa and across Asia. There are similarly high median maize yield losses for countries in Central America and the Caribbean, but only Chile

and Uruguay are badly affected in South America, and only Albania, Croatia and Greece in Europe. Median wheat yield losses per country are generally lower than for maize. Countries with median wheat losses higher than 5% are mostly in Asia and Europe. In Africa, annual median wheat yield losses higher than 5% are simulated in Ethiopia, Uganda and Tanzania, and in South America in Uruguay, Bolivia and Chile. These crop yield losses are modelled using the prevailing environment and management conditions in each country. Actual crop yield losses could only be determined based on an explicit spatial link between the extent of crop cultivation areas and areas vulnerable to water erosion, which would only be possible with on-site observations.

The distribution of the magnitude of crop yield losses and the share of grid cells affected by water erosion needs to be considered to assess each countries vulnerability to water erosion. In some large countries, the majority of cropland is exposed to low water erosion despite extensive vulnerable areas within the country. For example, large areas in the United States, Brazil, India and China are affected by water erosion. However, as these regions are only a small part of the entire cropland area, overall median crop losses are low. On the other hand, in some countries a small number of grid cells with high water erosion cause high median crop productivity losses. Afghanistan, Pakistan and Iran are ranked among the most vulnerable countries even though less than half of the grid cells are affected by water erosion under all scenarios.

In several countries, field management scenarios have a significant impact on the area affected by water erosion and on the magnitude of crop yield losses, as demonstrated by the uncertainty ranges in Figure 2. In most countries, the median maize and wheat yield losses are lowest with no tillage and cover crops and highest with conventional or reduced tillage and bare soil fallow. On a global scale, annual maize and wheat yield losses simulated under all field management scenarios range from 2–5% and 3–4%, respectively.

2.2 Fertilizer use and environmental drivers affect the impacts of water erosion

The simulated impact of water erosion on crop yields is strongly influenced by fertilizer input and environmental drivers in each country such as slope inclination and precipitation amount. Figure 3a shows that median maize and wheat yield losses per country tend to be higher in countries with higher levels of water erosion. Losses are relatively lower in countries with high rates of fertilizer application, which replace nutrients lost through soil runoff (Figure S10). We simulate a global median rate of nitrogen runoff from maize and wheat fields of 7 kg ha^{-1} yr^{-1} and 5 kg ha^{-1} yr^{-1}, and a global median rate of soil organic carbon runoff from maize and wheat fields of 107 kg ha^{-1} yr^{-1} and 72 kg ha^{-1} yr^{-1} during the whole simulation period (global maps on soil, nitrogen and carbon runoff are provided in the supplementary information in Figures S11–S13).

Slope steepness and precipitation strength are the most important environmental drivers influencing the impact of water erosion on crop yields. Figures 3b and 3c show how yield losses increase as a function of slope classes and rainfall erosivity classes[1]. The distribution of maize and wheat cropland in our grid cells per slope and rainfall erosivity classes is illustrated by the grey bars in the same plots. Around 73% of maize and wheat cropland is on slopes whose steepness does not exceed 5%. On those slopes, median global maize and wheat yield losses range from 0% to 1%. On steeper slopes, median yield losses range from 3% to 9%. Similarly, 69% of maize and wheat land is exposed to rainfall erosivity below 3000 MJ mm ha^{-1} h^{-1} yr^{-1}, which is the average rainfall erosivity on global cropland. For those areas, median crop yield losses range from 1% to 2%. Median crop yield losses on fields exposed to higher rainfall erosivity range from 2% to 4%.

The highest yield losses tend to occur in regions with low fertilizer input and high rates of water erosion. Figure 4 identifies agricultural regions susceptible to water erosion as indicated by

---

[1] Rainfall erosivity classes are taken from Panagos et al. (2017).

overlapping areas of slope steepness (IIASA/FAO, 2012) and rainfall erosivity (Panagos et al., 2017), and shows the average fertilizer application rates for maize- and wheat-producing countries (Mueller et al., 2012). Each map layer is presented in Figures S13–S15. Dark areas highlight most vulnerable locations characterised by high abundance of steep slopes in regions of high rainfall erosivity. These are most common in South, East and Southeast Asia, sub-Saharan Africa, and Latin America. The cultivation on steep slopes is a common factor of vulnerability outside the tropics as well, but rainfall erosivity decreases there, reducing the energy of rainfall to erode soil. Fertilizer application per country varies significantly. In most African countries and in several countries in Asia and Latin America, the fertilizer use is substantially lower than in the rest of the world.

2.3   The impact of water erosion on total maize and wheat production

By extrapolating average absolute maize and wheat yield losses across the entire irrigated and rainfed cultivation area of each crop in a grid cell, we sum the total annual production loss per country (Figure 5). We estimate that water erosion reduces the global production of maize and wheat by 9 million tonnes and 6 million tonnes annually. This accounts for less than 1% of the global average maize and wheat production of 1,091 million tonnes and 739 million tonnes, respectively, from 2013–2018 reported by FAOSTAT. Market values of the national maize and wheat production losses, derived by multiplying production losses with the average market prices ($ t^{-1}) in each country, add up to an annual global loss of approximately $2bn in maize production, and $1.3bn in wheat production. Highest production losses in absolute terms are in countries with the largest maize and wheat cultivation areas rather than in the most vulnerable countries. Tables 2 and 3 list the 20 countries with the highest annual reduction in maize and wheat production due to water erosion. These countries account for 84% and 77% of the global maize and wheat production.

We estimate the largest maize production declines for the most important producers such as Mexico, Brazil, United States, India, China and Indonesia. Nevertheless, losses in the United States and China are only 0.2% of their national production, but reach 5% of Mexico's

production. Few countries with the highest absolute losses have low shares of global production (e.g. Guatemala; Nicaragua; Nepal; Myanmar).

Similarly, the modelled loss of wheat production due to water erosion in absolute terms is highest for India and China as they produce nearly a third of global wheat production, but is less than 1% of their total production. High production losses in absolute terms for small producers are rarer than for maize. Countries with lowest production losses in absolute terms are most abundant in Africa, Southeast Asia and Latin America.

2.4 The Impact of uncertainty in field management and slope modelling

The impact of our assumption that the most common slope represents the whole grid cell is examined for Italy in Figure 6. The plots compare the distribution of modelled maize and wheat yield losses due to water erosion for cases in which all cropland is either on the most common slope class or on the flattest terrain in each grid cell. Median annual maize and wheat yield losses for the flattest terrain assumption are 0.2% and 1.2%, respectively, leading to annual maize and wheat production losses of 0.01 million tonnes and 0.04 million tonnes, respectively. For the most common slope scenario, median annual maize and wheat yield losses are 2.1% and 4.1%, with substantially higher annual maize and wheat production losses of 0.05 million tonnes and 0.1 million tonnes, respectively.

The uncertainty due to lacking field management information varies around the globe and is most pronounced in erosion-sensitive areas, where soil conservation techniques can reduce extreme water erosion rates considerably. In those areas, contrasting field management scenarios generate a large range of values with varying degrees of water erosion impacts on crop yields (Figure S17). We reduced this large uncertainty range in our baseline scenario by identifying and removing field management practices that are unlikely to be used in specific regions. However, due to the large variety of field management practices worldwide, we can only partly narrow down this uncertainty.

3 Discussion

3.1 Erosion-induced crop yield losses and fertilizer requirements for compensation

Previous studies suggest that soil loss rates up to 11 t ha^{-1} are tolerable to maintain crop productivity for soils in the United States (Schertz and Nearing, 2006) and in Europe (Panagos et al., 2018) based on the assumption that fertilizer will compensate for nutrient runoff. On fields with higher water erosion rates, Panagos et al. (2018) assumed that crop productivity would reduce by 8%, based on a review of relevant studies on erosion-crop productivity relationships. Similarly, our model outputs generate a median global reduction of maize and wheat yields of 6% for grid cells with water erosion of at least 11 t ha^{-1}. In fields with water erosion below 11 t ha^{-1} we simulate a considerably lower median crop yield reduction of 1%. However, large variations in fertilizer input between countries affect the impact of water erosion on crop yields. If fertilizer were not sufficiently supplied to compensate for nutrient losses in certain countries, their crop yield losses may be higher than in countries with both higher water erosion and fertilizer application rates (Balkovič et al., 2018). Although synthetic fertilizers can quickly compensate for nutrient loss, the recovery of lost organic matter and the consequent damage to soil structure can take decades (Poulton et al., 2018). Therefore, acceptable soil loss rates should not consider only the extent to which fertilizer application can replenish soil fertility. An assessment should also consider soil formation rates and off-site concerns such as the proximity to sensitive areas (Montgomery, 2007; Schertz and Nearing, 2006).

The additional fertilizer costs to compensate for water erosion can be higher than the loss of income due to production losses (Graves et al., 2015). Global median nitrogen runoff of 7 kg ha^{-1} yr^{-1} in maize fields and 5 kg ha^{-1} yr^{-1} in wheat fields, from our simulation outputs, would cost $1.7 ha^{-1} yr^{-1} and $1.2 ha^{-1} yr^{-1} [2]. The global annual nitrogen fertilizer replacement costs

---

[2] based on global urea price for the period 2015–2019 taken from World Bank (2020a).

for maize and wheat fields would be \$642m and \$255m, respectively. Although this is lower than the estimated annual maize and wheat production losses (\$2.0bn and \$1.3bn), replacement costs for lost nutrients would be considerably higher if we were to also account for phosphorus and potassium runoff. In addition, carbon runoff of median 107 kg ha^{-1} yr^{-1} and 72 kg ha^{-1} yr^{-1} in maize and wheat fields might add additional costs through nutrient replacement efforts such as manure application. On a global scale, the relative fertilizer replacement costs might be too low to incentivise farmers to introduce soil conservation measures, but they can be considerably higher for vulnerable areas (Hein, 2007). For a comprehensive assessment of water erosion impacts, off-site impacts on surrounding environments such as the pollution of surface water and emission of greenhouse gases also need to be considered (Chappell et al., 2016; Tilman et al., 2001). Several studies estimate higher costs of off-site impacts due to erosion than on-site costs through production losses and fertilizer replacement (Görlach et al., 2004; Graves et al., 2015). Further, we did not account for sediment re-distribution as we currently rely on simple water erosion models for global assessments. Topsoil accumulation in deposition areas may improve nutrient availability and soil properties and can offset the negative effects on crops in eroded areas (Bakker et al., 2007; Duan et al., 2016).

Due to the high fertilizer use in major maize and wheat production areas, which are mostly located on flat terrain and in regions with lower rainfall erosivity than the global average, water erosion has had a low impact on annual global production losses in absolute terms. Vulnerable regions with potentially high crop yield losses are mostly outside major production regions and therefore they hardly affect changes in global maize and wheat production. Den Biggelaar et al. (2004a) also estimated a low impact of water erosion on a global scale, and concluded that the small losses would likely be masked over the short term by market fluctuations, weather, and other environmental perturbations. Furthermore, market mechanisms such as trade flows can considerably reduce production losses. Sartori et al. (2019) used a global market simulation model that accounted for market impacts of soil erosion, which reduced direct

production losses by three times. Nevertheless, as erosion impacts are cumulative, they may cause more serious losses if erosion continues unabated over a long period of time (Den Biggelaar et al., 2004a), and could ultimately lead to total topsoil loss and the land being abandoned. Moreover, water erosion could be self-reinforcing, by decreasing the protective cover through reduced crop cover and residues on the soil surface (Ponzi, 1993).

Slope inclination and precipitation intensity are the dominant environmental characteristics affecting water erosion. Soil types are generally relevant in GGCM crop yield simulations (Folberth et al., 2016) and for erosion-productivity relationships (den Biggelaar et al., 2001; Lal, 1995), but on a global scale their impact on water erosion is small compared to slope steepness and precipitation. This means water erosion impacts are highest in hilly areas, in the tropics and in other regions with heavy precipitation. In countries with diverse environmental conditions, the variation in water erosion impacts is usually wide ranging and therefore a comparison of the extent of cropland vulnerable to water erosion should be further analysed on a sub-national scale.

3.2   Potential impacts of water erosion on livelihoods

High production losses from water erosion on a national or regional scale can severely impact livelihoods of farmers (Wynants et al., 2019). The agricultural sector of both sub-Sahran Africa and South Asia contributes roughly 16% to their GDP, compared to a worldwide share of approximately 4% (World Bank, 2020b). Moreover, food security is a pressing issue in those regions (von Grebmer et al., 2012). Whilst in some of these regions water erosion was recently reduced through programs improving land management (Nyssen et al., 2015), increasing crop demand through population growth and market effects led to re-cultivation of tropical steep slopes (Turkelboom et al., 2008) or soils prone to degradation (Wildemeersch et al., 2015). Pressures are likely to increase through climate change impacts on agriculture, which are projected to decrease agricultural productivity highest in low latitudes (Iizumi et al., 2017; Rosenzweig et al., 2014), which will likely enhance food security issues (Knox et al., 2012; Wheeler and Von Braun, 2013). The impact of climate change on water erosion impacts is still

unclear but projected increases in rainfall intensity (Olsson et al., 2019; Wang et al., 2014) and diminishing vegetation cover through increasing temperature (Zhao et al., 2017) may accelerate water erosion and its impacts on crop yields (Li and Fang, 2016). Our simulation results indicate that several countries in regions most affected by food security issues today and projected to be under high pressure by population growth and climate change in the future are among the most affected by high relative production losses due to water erosion.

3.3 Uncertainties in water erosion estimates

The large spatial resolution of global-gridded crop models cause uncertainty from various input sources including climate, soil, field management, distribution of crop cultivars and cropland, irrigation area, growing seasons, model structure and model parameterization, most of which have been addressed by prior studies (Folberth et al., 2016, 2019; Mueller et al., 2017; Porwollik et al., 2017). In this study, we focus on the uncertainty from cultivated slope and field management data, as both are critical for estimating water erosion and its effect on crop yields and production.

3.3.1 Uncertain slopes of modelled fields

Slope data is the most critical parameter for estimating water erosion. However, the uncertainty of global land use datasets (Fritz et al., 2015; Lesiv et al., 2019) does not enable us to establish explicit spatial links between maize and wheat cultivation areas and slopes without on-site observations. Instead, we use the slope covering the largest area in a grid cell to capture the slope most likely covered by most of the cropland. This approach represents the prevailing topographic differences of global crop production regions but cannot capture the heterogeneity of fields in certain areas. In an ideal situation where all cultivated areas are concentrated on the flattest terrain available, simulated water erosion impacts on crop yields are reduced substantially. However, the distribution of cropland is based on more factors than the topography of land, such as the suitability of soil, climate and socio- economic circumstances or limitations such as land tenure and competing land use (Hazell and Wood, 2008; Nyssen et al., 2019).

3.3.2 Uncertainties in field management

Field management can vary substantially between regions, farming systems and farmers, and is based on a complex web of factors (Pannell et al., 2014). While our management scenarios bracket the range of field management intensities and soil surface coverage, our baseline scenario narrows down prevailing field management by selecting or excluding scenarios based on environmental- and country-specific indicators. Apart from similar approaches (e.g. Porwollik et al., 2019), no detailed representation of the diversity in global field management currently exists. Moreover, our field management scenarios are constant for every season and we do not account for the farmer's actions to mitigate soil erosion, which might significantly reduce water erosion impacts (Tiffen et al., 1994).

Yet an advantage of simulating constant field management is that it enables us to detect the impact of water erosion on soil resources in the long term, which might otherwise have been masked by technological advances such as higher yielding crop varieties, herbicides, insecticides, new planting technologies, and increased fertilizer input to compensate for sediment runoff (Littleboy et al., 1996). Moreover, we can address the likely differences in water erosion impacts with different intensities of field management, as our model outputs reflect the ability of cover crops, crop residues and low tillage intensity to decrease water erosion rates and to maintain and replenish soil nutrients. Although this reduces crop yield losses due to water erosion, it does not necessarily translate into higher crop yields due to other growth constraints being influenced by the choice of farming techniques. Since field management practices greatly influence crop yields in general, and water erosion in particular, improving their representation and understanding the decision processes of farmers responding to changing physical conditions in their fields would help to improve our understanding of water erosion impacts on crop yields.

3.3.3 Data requirements to improve global erosion impact assessments

Future global studies on water erosion impacts may benefit from current efforts to compile spatial data on representative management practices such as tillage systems (Porwollik et al.,

2019), and remote sensing products for spatial attribution of field management practices (Hively et al., 2018; Zheng et al., 2014). In addition, the increasing availability of high-resolution data through improvements in remote sensing techniques will benefit future global water erosion assessments (Buchhorn et al., 2020). However, due to the current uncertainties in global land use maps (Lesiv et al., 2019) and spatial field management data (Folberth et al., 2019), global studies cannot replace field-scale assessments based on precise information on management practices and site characteristics. Due to higher spatial detail, field-scale assessments can be based on more complex water erosion models, which may include special elements such as channels and ponds to identify potential sources and sinks of sediments and associated nutrients within a field (Jetten et al., 2003). By including depositional areas within the spatial unit studied, positive effects of topsoil accumulation on crop productivity can be considered (Bakker et al., 2007). In addition, studies based on data with a higher temporal resolution can consider the impact of individual rainfall events on sediment runoff instead of focusing on average erosion rates as it is common in global studies. In other words, smaller-scale studies can more precisely inform about actual water erosion impacts on a field to support effective anti-erosion measures on-site. However, studies on erosion-productivity relationships cannot normally be scaled-up as the robustness of locally observed relationships need to be re-evaluated for different environmental and socioeconomic conditions in each location. Given the current lack of consistent field studies representing all global environments, a bottom-up approach to deliver large-scale indicators on erosion rates and impacts to inform agricultural and environmental policy programs is not currently feasible (Alewell et al., 2019).

The limited availability of global experimental field-scale data means that only simple erosion models are appropriate for global studies. For this reason, USLE-based models have been chosen in this study and by most other recent global studies to estimate water erosion rates at large scales (Borrelli et al., 2017; Naipal et al., 2018). In a previous study, we tested the robustness of our modelling approach and concluded that water erosion rates simulated with

EPIC-IIASA largely overlapped with experimentally-measured erosion rates in most global cropland environments, while water erosion rates simulated at locations with steep slopes and strong precipitation were overestimated (Carr et al., 2020). A major challenge in the evaluation of simulated water erosion rates was the limited amount of appropriate field data, which do not represent all needed regions and field management scenarios, as well as the inconsistency in field experiment setups. Whilst the robustness of spatial patterns of crop yields simulated with EPIC-IIASA has been evaluated using regional yield statistics and other global crop and land use models as a part of ISI-MIP and GGCMI model inter-comparison initiatives (Mueller et al., 2017), similar comprehensive evaluation and benchmarking techniques to improve global water erosion models are hampered by a lack of appropriate field data. Recent efforts to collate erosion measurements and metadata from existing studies may improve the global coverage of appropriate field data in the future (Benaud et al., 2020; Borrelli et al., 2020). In addition to the need for more spatial data on representative management practices and higher-resolution datasets on land use patterns and topography, a more consistent approach to field-based data collection to evaluate model outputs would enable such studies to be used in future large-scale water erosion assessments.

4 Conclusion

We used a global gridded crop model to analyse the vulnerability of maize and wheat producing regions to water erosion. Locations that are highly vulnerable to water erosion are concentrated in regions combining hilly terrain, strong precipitation and low fertilizer inputs. But water erosion has only a small impact on global maize and wheat production, because the major maize and wheat production areas are on relatively flat terrain and nutrient losses through water erosion are offset by high fertilizer applications. However, this compensation of soil loss with fertilizers to maintain crop yields hides the negative impacts of water erosion on soil resources and surrounding environments.

We have performed a globally-consistent and transparent analysis of water erosion impacts on maize and wheat production. The most crucial data requirements to improve the robustness of simulated water erosion impacts on global crops include well-defined field data covering all global regions to evaluate water erosion estimates, higher-resolution global land use datasets and detailed information on field management patterns. Improving our understanding of soil conservation and anti-erosion measures used in each region when cultivating slopes would enable us to improve our representation of vulnerable regions. As these datasets are currently not available in higher detail at the global scale, further research on water erosion impacts could focus on the most vulnerable regions by analysing land use patterns and all environmental circumstances on-site at a finer resolution. The high vulnerability to water erosion in sub-Saharan Africa, and parts of South Asia and Latin America, where future changes in population growth and climate could amplify land degradation processes, are priorities for further research.

References

Alewell, C., Borrelli, P., Meusburger, K. and Panagos, P.: Using the USLE: Chances, challenges and limitations of soil erosion modelling, Int. Soil Water Conserv. Res., 7(3), 203–225, doi:10.1016/j.iswcr.2019.05.004, 2019.

Bakker, M. M., Govers, G. and Rounsevell, M. D. A.: The crop productivity – erosion relationship : an analysis based on experimental work, Catena, 57, 55–76, doi:10.1016/j.catena.2003.07.002, 2004.

Bakker, M. M., Govers, G., Jones, R. A. and Rounsevell, M. D. A.: The effect of soil erosion on Europe's crop yields, Ecosystems, 10(7), 1209–1219, doi:10.1007/s10021-007-9090-3, 2007.

Balkovič, J., van der Velde, M., Skalský, R., Xiong, W., Folberth, C., Khabarov, N., Smirnov, A., Mueller,

N. D. and Obersteiner, M.: Global wheat production potentials and management flexibility under the representative concentration pathways, Glob. Planet. Change, 122, 107–121, doi:10.1016/j.gloplacha.2014.08.010, 2014.

Balkovič, J., Skalský, R., Folberth, C., Khabarov, N., Schmid, E., Madaras, M., Obersteiner, M. and van der Velde, M.: Impacts and Uncertainties of +2°C of Climate Change and Soil Degradation on European Crop Calorie Supply, Earth's Futur., 6(3), 373–395, doi:10.1002/2017EF000629, 2018.

Benaud, P., Anderson, K., Evans, M., Farrow, L., Glendell, M., James, M. R., Quine, T. A., Quinton, J. N., Rawlins, B., Jane Rickson, R. and Brazier, R. E.: National-scale geodata describe widespread accelerated soil erosion, Geoderma, 371, 114378, doi:10.1016/j.geoderma.2020.114378, 2020.

den Biggelaar, C., Lal, R., Wiebe, K. and Breneman, V.: Impact of soil erosion on crop yields in North America, Adv. Agron., 72, 1–52, doi:10.1016/s0065-2113(01)72010-x, 2001.

Den Biggelaar, C., Lal, R., Wiebe, K., Eswaran, H., Breneman, V. and Reich, P.: The Global Impact Of Soil Erosion On Productivity*. II: Effects On Crop Yields And Production Over Time, Adv. Agron., 81(03), 49–95, doi:10.1016/S0065-2113(03)81002-7, 2004a.

Den Biggelaar, C., Lal, R., Wiebe, K. and Breneman, V.: The Global Impact of Soil Erosion on Productivity, Adv. Agron., 81(03), 1–4, doi:10.1016/S0065-2113(03)81001-5, 2004b.

van den Born, G. J., de Haan, B. J., Pearche, D. W. and Howarth, A.: Technical Report on Soil Degradation in Europe: an integrated economic and environmental assessment., 2000.

Borrelli, P., Robinson, D. A., Fleischer, L. R., Lugato, E., Ballabio, C., Alewell, C., Meusburger, K., Modugno, S., Schütt, B., Ferro, V., Bagarello, V., Oost, K. Van, Montanarella, L. and Panagos, P.: An assessment of the global impact of 21st century land use change on soil erosion, Nat. Commun., 8(1), 1–13, doi:10.1038/s41467-017-02142-7, 2017.

Borrelli, P., Alewell, C., Alvarez, P., Anache, J. A. A., Baartman, J., Ballabio, C., Bezak, N., Biddoccu, M., Cerdà, A., Chalise, D., Chen, S., Chen, W., Girolamo, A. M. De, Gessesse, G. D., Deumlich, D., Diodato, N., Efthimiou, N., Erpul, G., Fiener, P., Freppaz, M., Gentile, F., Gericke, A., Haregeweyn, N., Hu, B., Jeanneau, A., Kaffas, K., Kiani-Harchegani, M., Villuendas, I. L., Li, C., Lombardo, L., López-Vicente, M., Lucas-Borja, M. E., Märker, M., Miao, C., Mikoš, M., Modugno, S., Möller, M., Naipal, V., Nearing, M., Owusu, S., Panday, D., Patault, E., Patriche, C. V., Poggio, L., Portes, R., Quijano, L., Rahdari, M. R., Renima, M., Ricci, G. F., Rodrigo-Comino, J., Saia, S., Samani, A. N., Schillaci, C., Syrris, V., Kim, H. S., Spinola, D. N., Oliveira, P. T., Teng, H., Thapa, R., Vantas, K., Vieira, D., Yang, J. E., Yin, S., Zema, D. A., Zhao, G. and Panagos, P.: Earth-Science Reviews Soil erosion modelling : A global review and statistical analysis, EarthArxiv (preprint), 2020.

Buchhorn, M., Lesiv, M., Tsendbazar, N. E., Herold, M., Bertels, L. and Smets, B.: Copernicus global land cover layers-collection 2, Remote Sens., 12(6), 1–14, doi:10.3390/rs12061044, 2020.

Carr, T., Balkovič, J., Dodds, P., Folberth, C., Fulajtar, E. and Skalsky, R.: Uncertainties, sensitivities and robustness of simulated water erosion in an EPIC-based global-gridded crop model,

Biogeosciences, 17, 5263–5283, doi:10.5194/bg-2020-93, 2020.

Chappell, A., Baldock, J. and Sanderman, J.: The global significance of omitting soil erosion from soil organic carbon cycling schemes, Nat. Clim. Chang., 6(2), 187–191, doi:10.1038/nclimate2829, 2016.

Chung, S. W., Gassman, P. W., Kramer, L. A., Williams, J. R., Gu, R. R., Chung, S. W. ;, Gassman, P. W. ;, Kramer, L. A. ; and Williams, J. R. ; Validation of EPIC for Two Watersheds in Southwest Iowa Recommended Citation Validation of EPIC for Two Watersheds in Southwest Iowa, 1999.

Doetterl, S., Van Oost, K. and Six, J.: Towards constraining the magnitude of global agricultural sediment and soil organic carbon fluxes, Earth Surf. Process. Landforms, 37(6), 642–655, doi:10.1002/esp.3198, 2012.

Duan, X., Liu, B., Gu, Z., Rong, L. and Feng, D.: Quantifying soil erosion effects on soil productivity in the dry-hot valley, southwestern China, Environ. Earth Sci., 75(16), 1–9, doi:10.1007/s12665-016-5986-6, 2016.

Elliott, J., Deryng, D., Müller, C., Frieler, K., Konzmann, M., Gerten, D., Glotter, M., Flörke, M., Wada, Y., Best, N., Eisner, S., Fekete, B. M., Folberth, C., Foster, I., Gosling, S. N., Haddeland, I., Khabarov, N., Ludwig, F., Masaki, Y., Olin, S., Rosenzweig, C., Ruane, A. C., Satoh, Y., Schmid, E., Stacke, T., Tang, Q. and Wisser, D.: Constraints and potentials of future irrigation water availability on agricultural production under climate change, Proc. Natl. Acad. Sci. U. S. A., 111(9), 3239–3244, doi:10.1073/pnas.1222474110, 2014.

Enters, T.: Methods for the economic assessment of the on- and off-site impacts of soil erosion., 1998.

FAO: AQUASTAT Main Database. available at: http://www.fao.org/nr/water/aquastat/data (last access: 08.03.2021), [online] Available from: http://www.fao.org/nr/water/aquastat/data/query/index.html?lang=en (Accessed 1 September 2020), 2016.

FAO: FAOSTAT. available at: http://www.fao.org/faostat/en/#data (last access: 08.03.2021), [online] Available from: http://www.fao.org/faostat/en/#data, 2020.

FAO and ITPS: Status of the World's Soil Resources (SWSR) - Main Report, Rome., 2015.

Folberth, C., Skalský, R., Moltchanova, E., Balkovič, J., Azevedo, L. B., Obersteiner, M. and van der Velde, M.: Uncertainty in soil data can outweigh climate impact signals in global crop yield simulations, Nat. Commun., 7(May), 11872, doi:10.1038/ncomms11872, 2016.

Folberth, C., Elliott, J., Müller, C., Balkovič, J., Chryssanthacopoulos, J., Izaurralde, R. C., Jones, C. D., Khabarov, N., Liu, W., Reddy, A., Schmid, E., Skalský, R., Yang, H., Arneth, A., Ciais, P., Deryng, D., Lawrence, P. J., Olin, S., Pugh, T. A. M., Ruane, A. C. and Wang, X.: Parameterization-induced uncertainties and impacts of crop management harmonization in a global gridded crop model ensemble, PLoS One, 14(9), e0221862, doi:10.1371/journal.pone.0221862, 2019.

Fritz, S., See, L., Mccallum, I., You, L., Bun, A., Moltchanova, E., Duerauer, M., Albrecht, F., Schill, C.,

Perger, C., Havlik, P., Mosnier, A., Thornton, P., Wood-Sichra, U., Herrero, M., Becker-Reshef, I., Justice, C., Hansen, M., Gong, P., Abdel Aziz, S., Cipriani, A., Cumani, R., Cecchi, G., Conchedda, G., Ferreira, S., Gomez, A., Haffani, M., Kayitakire, F., Malanding, J., Mueller, R., Newby, T., Nonguierma, A., Olusegun, A., Ortner, S., Rajak, D. R., Rocha, J., Schepaschenko, D., Schepaschenko, M., Terekhov, A., Tiangwa, A., Vancutsem, C., Vintrou, E., Wenbin, W., van der Velde, M., Dunwoody, A., Kraxner, F. and Obersteiner, M.: Mapping global cropland and field size, Glob. Chang. Biol., 21(5), 1980–1992, doi:10.1111/gcb.12838, 2015.

García-Ruiz, J. M., Beguería, S., Nadal-Romero, E., González-Hidalgo, J. C., Lana-Renault, N. and Sanjuán, Y.: A meta-analysis of soil erosion rates across the world, Geomorphology, 239, 160–173, doi:10.1016/j.geomorph.2015.03.008, 2015.

Gibbs, H. K. and Salmon, J. M.: Mapping the world's degraded lands, Appl. Geogr., 57, 12–21, doi:10.1016/j.apgeog.2014.11.024, 2015.

Görlach, B., Landgrebe-trinkunaite, R., Interwies, E., Bouzit, M., Darmendrail, D. and Rinaudo, J.: Assessing the Economic Impacts of Soil Degradation - Final Report Volume III, , IV(December), 1–31, 2004.

Graves, A. R., Morris, J., Deeks, L. K., Rickson, R. J., Kibblewhite, M. G., Harris, J. A., Farewell, T. S. and Truckle, I.: The total costs of soil degradation in England and Wales, Ecol. Econ., 119, 399–413, doi:10.1016/j.ecolecon.2015.07.026, 2015.

von Grebmer, K., Ringler, C., Rosegrant, M. W., Olofinbiyi, T., Wiesmann, D., Fritschel, H., Badiane, O., Torero, M., Yohannes, Y., Thompson, J., von Oppeln, C. and Rahall, J.: 2012 Global hunger index: The challenege of hunger: Ensuring sustainable food security under land, water, and energy stresses., Bonn; Dublin; Washington, D.C., 2012.

Hazell, P. and Wood, S.: Drivers of change in global agriculture, Philos. Trans. R. Soc. B Biol. Sci., 363(1491), 495–515, doi:10.1098/rstb.2007.2166, 2008.

Hein, L.: Assessing the costs of land degradation: a case study for the puentes catchment, southeast Spain, L. Degrad. Dev., 18, 631–642, 2007.

Hively, W. D., Lamb, B. T., Daughtry, C. S. T., Shermeyer, J., McCarty, G. W. and Quemada, M.: Mapping crop residue and tillage intensity using WorldView-3 satellite shortwave infrared residue indices, Remote Sens., 10(10), doi:10.3390/rs10101657, 2018.

IIASA/FAO: Global Agro-ecological Zones (GAEZ v3.0), IIASA, Laxenburg, Austria and FAO, Rome, Italy., 2012.

Iizumi, T., Furuya, J., Shen, Z., Kim, W., Okada, M., Fujimori, S., Hasegawa, T. and Nishimori, M.: Responses of crop yield growth to global temperature and socioeconomic changes, Sci. Rep., 7(1), 1–10, doi:10.1038/s41598-017-08214-4, 2017.

Izaurralde, R. C., Williams, J. R., McGill, W. B., Rosenberg, N. J. and Jakas, M. C. Q.: Simulating soil

C dynamics with EPIC: Model description and testing against long-term data, Ecol. Modell., 192(3–4), 362–384, doi:10.1016/j.ecolmodel.2005.07.010, 2006.

Jetten, V., Govers, G. and Hessel, R.: Erosion models: Quality of spatial predictions, Hydrol. Process., 17(5), 887–900, doi:10.1002/hyp.1168, 2003.

Knox, J., Hess, T., Daccache, A. and Wheeler, T.: Climate change impacts on crop productivity in Africa and South Asia, Environ. Res. Lett., 7(3), 034032, doi:10.1088/1748-9326/7/3/034032, 2012.

Kottek, M., Grieser, J., Beck, C., Rudolf, B. and Rubel, F.: World Map of the Köppen-Geiger climate classification updated, Meteorol. Zeitschrift, 15(3), 259–263, doi:10.1097/00041433-200208000-00008, 2006.

De la Rosa, D., Moreno, J. A., Mayol, F. and Bonsón, T.: Assessment of soil erosion vulnerability in western Europe and potential impact on crop productivity due to loss of soil depth using the Impe1ERO model, Agric. Ecosyst. Environ., 81(3), 179–190, doi:10.1016/S0167-8809(00)00161-4, 2000.

Lal, R.: Erosion-crop productivity relationships for soils of Africa, Soil Sci. Soc. Am. J., 59(3), 661–667, doi:10.2136/sssaj1995.03615995005900030004x, 1995.

Larney, F. J., Janzen, H. H., Olson, B. M. and Olson, A. F.: Erosion-productivity-soil amendment relationships for wheat over 16 years, Soil Tillage Res., 103(1), 73–83, doi:10.1016/j.still.2008.09.008, 2009.

Lesiv, M., Laso Bayas, J. C., See, L., Duerauer, M., Dahlia, D., Durando, N., Hazarika, R., Kumar Sahariah, P., Vakolyuk, M., Blyshchyk, V., Bilous, A., Perez-Hoyos, A., Gengler, S., Prestele, R., Bilous, S., Akhtar, I. ul H., Singha, K., Choudhury, S. B., Chetri, T., Malek, Ž., Bungnamei, K., Saikia, A., Sahariah, D., Narzary, W., Danylo, O., Sturn, T., Karner, M., McCallum, I., Schepaschenko, D., Moltchanova, E., Fraisl, D., Moorthy, I. and Fritz, S.: Estimating the global distribution of field size using crowdsourcing, Glob. Chang. Biol., 25(1), 174–186, doi:10.1111/gcb.14492, 2019.

Li, Z. and Fang, H.: Impacts of climate change on water erosion: A review, Earth-Science Rev., 163, 94–117, doi:10.1016/j.earscirev.2016.10.004, 2016.

Littleboy, M., Cogle, A. L., Smith, G. D., Rao, C. K. P. C. and Yule, D. F.: Soil management and production of Alfisols in the semi-arid tropics. IV. Simulation of decline in productivity caused by soil erosion, Aust. J. Soil Res., 34(1), 127–138, doi:10.1071/SR9960127, 1996.

Montanarella, L.: Trends in Land Degradation in Europe, in Climate and Land Degradation, edited by M. V. K. Sivakumar and N. Ndiang'ui, pp. 83–104, Springer Berlin Heidelberg, Berlin, Heidelberg., 2007.

Montanarella, L., Pennock, D. J., McKenzie, N., Badraoui, M., Chude, V., Baptista, I., Mamo, T., Yemefack, M., Aulakh, M. S., Yagi, K., Hong, S. Y., Vijarnsorn, P., Zhang, G. L., Arrouays, D., Black, H., Krasilnikov, P., Sobocká, J., Alegre, J., Henriquez, C. R., Mendonça-Santos, M. de L., Taboada, M., Espinosa-Victoria, D., AlShankiti, A., AlaviPanah, S. K., Mustafa Elsheikh, E. A. El, Hempel, J., Arbestain, M. C., Nachtergaele, F. and Vargas, R.: World's soils are under threat, Soil, 2(1), 79–82,

doi:10.5194/soil-2-79-2016, 2016.

Montgomery, D. R.: Soil erosion and agricultural sustainability., Proc. Natl. Acad. Sci. U. S. A., 104(33), 13268–72, doi:10.1073/pnas.0611508104, 2007.

Mueller, C., Elliott, J., Chryssanthacopoulos, J., Arneth, A., Balkovic, J., Ciais, P., Deryng, D., Folberth, C., Glotter, M., Hoek, S., Iizumi, T., Izaurralde, R. C., Jones, C., Khabarov, N., Lawrence, P., Liu, W., Olin, S., Pugh, T. A. M., Ray, D. K., Reddy, A., Rosenzweig, C., Ruane, A. C., Sakurai, G., Schmid, E., Skalsky, R., Song, C. X., Wang, X., De Wit, A. and Yang, H.: Global gridded crop model evaluation: Benchmarking, skills, deficiencies and implications, Geosci. Model Dev., 10(4), 1403–1422, doi:10.5194/gmd-10-1403-2017, 2017.

Mueller, N. D., Gerber, J. S., Johnston, M., Ray, D. K., Ramankutty, N. and Foley, J. A.: Closing yield gaps through nutrient and water management, Nature, 494(7437), 390–390, doi:10.1038/nature11907, 2012.

Nachtergaele, F. O., Petri, M., Biancalani, R., van Lynden, G., van Velthuizen, H. and Bloise, M.: Global Land Degradation Information System (GLADIS) - An Information database for Land Degradation Assessment at Global Level, Management, (September), 110, 2011.

Naipal, V., Ciais, P., Wang, Y., Lauerwald, R., Guenet, B. and Van Oost, K.: Global soil organic carbon removal by water erosion under climate change and land use change during AD-1850-2005, Biogeosciences, 15(14), 4459–4480, doi:10.5194/bg-15-4459-2018, 2018.

Nelson, G. C., Valin, H., Sands, R. D., Havlík, P., Ahammad, H., Deryng, D., Elliott, J., Fujimori, S., Hasegawa, T., Heyhoe, E., Kyle, P., Von Lampe, M., Lotze-Campen, H., Mason D'Croz, D., Van Meijl, H., Van Der Mensbrugghe, D., Müller, C., Popp, A., Robertson, R., Robinson, S., Schmid, E., Schmitz, C., Tabeau, A. and Willenbockel, D.: Climate change effects on agriculture: Economic responses to biophysical shocks, Proc. Natl. Acad. Sci. U. S. A., 111(9), 3274–3279, doi:10.1073/pnas.1222465110, 2014.

Nelson, R. A., Dimes, J. P., Silburn, D. M. and Carberry, P. S.: Erosion/ productivity modelling of maize farming in the Philippine uplands. Part I: a simple description of the agricultural production systems simulator. SEARCA-UQ Uplands Research Project. Working Paper No. 12., Los Baños., 1996.

Nkonya, E., Gerber, N., Baumgartner, P., Braun, J. Von, Pinto, A. De, Graw, V., Kato, E., Kloos, J. and Walter, T.: The Economics of Desertification, Land Degradation, and Drought Toward an Integrated Global Assessment, Lang., 2011.

Nyssen, J., Frankl, A., Zenebe, A., Deckers, J. and Poesen, J.: Land Management in the Northern Ethiopian Highlands: Local and Global Perspectives; Past, Present and Future, L. Degrad. Dev., 26(7), 759–764, doi:10.1002/ldr.2336, 2015.

Nyssen, J., Tielens, S., Gebreyohannes, T., Araya, T., Teka, K., van de Wauw, J., Degeyndt, K., Descheemaeker, K., Amare, K., Haile, M., Zenebe, A., Munro, N., Walraevens, K., Gebrehiwot, K., Poesen, J., Frankl, A., Tsegay, A. and Deckers, J.: Understanding spatial patterns of soils for

sustainable agriculture in northern Ethiopia's tropical mountains., 2019.

Oldeman, L. R., Hakkeling, R. T. and Sombroek, G.: Status of Human-Induced Soil Degradation 2nd ed., Wageningen., 1991.

Olsson, L., Barbosa, H., Bhadwal, S., Cowie, A., Delusca, K., Flores-Renteria, D., Hermans, K., Jobbagy, E., Kurz, W., Li, D., Sonwa, D. J. and Stringer, L.: Land Degradation, in Climate Change and Land: an IPCC special report on climate change, desertification, land degradation, sustainable land management, food security, and greenhouse gas fluxes in terrestrial ecosystems, edited by .R. Shukla, J. Skea, E. C. Buendia, V. Masson-Delmotte, H.-O. Pörtner, D. C. Roberts, P. Zhai, R. Slade, S. Connors, R. van Diemen, M. Ferrat, E. Haughey, S. Luz, S. Neogi, M. Pathak, J. Petzold, J. P. Pereira, P. Vyas, E. Huntley, K. Kissick, M.Belkacemi, and J. Malley., 2019.

Oyedele, D. J. and Aina, P. O.: A study of soil factors in relation to erosion and yield of maize on a Nigerian soil, Soil Tillage Res., 48(1–2), 115–125, doi:10.1016/S0167-1987(98)00110-X, 1998.

Panagos, P., Imeson, A., Meusburger, K., Borrelli, P., Poesen, J. and Alewell, C.: Soil Conservation in Europe: Wish or Reality?, L. Degrad. Dev., 27(6), 1547–1551, doi:10.1002/ldr.2538, 2016.

Panagos, P., Borrelli, P., Meusburger, K., Yu, B., Klik, A., Lim, K. J., Yang, J. E., Ni, J., Miao, C., Chattopadhyay, N., Sadeghi, S. H., Hazbavi, Z., Zabihi, M., Larionov, G. A., Krasnov, S. F., Gorobets, A. V., Levi, Y., Erpul, G., Birkel, C., Hoyos, N., Naipal, V., Oliveira, P. T. S., Bonilla, C. A., Meddi, M., Nel, W., Dashti, H. Al, Boni, M., Diodato, N., Van Oost, K., Nearing, M. and Ballabio, C.: Global rainfall erosivity assessment based on high-temporal resolution rainfall records, Sci. Rep., 7(June), 1–12, doi:10.1038/s41598-017-04282-8, 2017.

Panagos, P., Standardi, G., Borrelli, P., Lugato, E., Montanarella, L. and Bosello, F.: Cost of agricultural productivity loss due to soil erosion in the European Union: From direct cost evaluation approaches to the use of macroeconomic models, L. Degrad. Dev., 29(3), 471–484, doi:10.1002/ldr.2879, 2018.

Pannell, D. J., Llewellyn, R. S. and Corbeels, M.: The farm-level economics of conservation agriculture for resource-poor farmers, Agric. Ecosyst. Environ., 187, 52–64, doi:10.1016/j.agee.2013.10.014, 2014.

Pimentel, D., Harvey, C., Resosudarmo, P., Sinclair, K., Kurz, D., McNair, M., Crist, S., Shpritz, L., Fitton, L., Saffouri, R. and Blair, R.: Environmental and economic costs of soil erosion and conservation benefits., Science (80-.)., 267(5201), 1117–1123, doi:10.1126/science.267.5201.1117, 1995.

Poesen, J.: Soil erosion in the Anthropocene: Research needs, Earth Surf. Process. Landforms, 43(1), 64–84, doi:10.1002/esp.4250, 2018.

Ponzi, D.: Soil erosion and productivity: A brief review, Desertif. Bull. 22, 22, 36–44, 1993.

Portmann, F. T., Siebert, S. and Döll, P.: MIRCA2000—Global monthly irrigated and rainfed crop areas around the year 2000: A new high-resolution data set for agricultural and hydrological modeling, Global Biogeochem. Cycles, 24(1), doi:10.1029/2008GB003435, 2010.

Porwollik, V., Müller, C., Elliott, J., Chryssanthacopoulos, J., Iizumi, T., Ray, D. K., Ruane, A. C., Arneth,

A., Balkovič, J., Ciais, P., Deryng, D., Folberth, C., Izaurralde, R. C., Jones, C. D., Khabarov, N., Lawrence, P. J., Liu, W., Pugh, T. A. M., Reddy, A., Sakurai, G., Schmid, E., Wang, X., de Wit, A. and Wu, X.: Spatial and temporal uncertainty of crop yield aggregations, Eur. J. Agron., 88, 10–21, doi:10.1016/j.eja.2016.08.006, 2017.

Porwollik, V., Rolinski, S., Heinke, J. and Müller, C.: Generating a rule-based global gridded tillage dataset, Earth Syst. Sci. Data, 11(2), 823–843, doi:10.5194/essd-11-823-2019, 2019.

Poulton, P., Johnston, J., Macdonald, A., White, R. and Powlson, D.: Major limitations to achieving "4 per 1000" increases in soil organic carbon stock in temperate regions: Evidence from long-term experiments at Rothamsted Research, United Kingdom, Glob. Chang. Biol., 24(6), 2563–2584, doi:10.1111/gcb.14066, 2018.

Rosenzweig, C., Elliott, J., Deryng, D., Ruane, A. C., Müller, C., Arneth, A., Boote, K. J., Folberth, C., Glotter, M., Khabarov, N., Neumann, K., Piontek, F., Pugh, T. A. M., Schmid, E., Stehfest, E., Yang, H. and Jones, J. W.: Assessing agricultural risks of climate change in the 21st century in a global gridded crop model intercomparison, Proc. Natl. Acad. Sci., 111(9), 3268–3273, doi:10.1073/pnas.1222463110, 2014.

Ruane, A. C., Goldberg, R. and Chryssanthacopoulos, J.: Climate forcing datasets for agricultural modeling: Merged products for gap-filling and historical climate series estimation, Agric. For. Meteorol., 200, 233–248, doi:10.1016/j.agrformet.2014.09.016, 2015.

Sacks, W. J., Deryng, D., Foley, J. A. and Ramankutty, N.: Crop planting dates: An analysis of global patterns, Glob. Ecol. Biogeogr., 19(5), 607–620, doi:10.1111/j.1466-8238.2010.00551.x, 2010.

Sartori, M., Philippidis, G., Ferrari, E., Borrelli, P., Lugato, E., Montanarella, L. and Panagos, P.: A linkage between the biophysical and the economic: Assessing the global market impacts of soil erosion, Land use policy, 86(December 2018), 299–312, doi:10.1016/j.landusepol.2019.05.014, 2019.

Schertz, D. L. and Nearing, M. A.: Erosion Tolerance / Soil Loss Tolerance, in Encyclopedia of Soil Science, edited by R. Lal, pp. 640–624., 2006.

Sharpley, A. N. and Williams, J. R.: EPIC — Erosion / Productivity Impact Calculator: 1. Model Documentation, U.S. Dep. Agric. Tech. Bull., 1768, 235, 1990.

Tiffen, M., Mortimore, M. and Gichuki, F.: More people, less erosion: environmental recovery in Kenya, J. Wiley. [online] Available from: https://books.google.co.uk/books?id=dinbAAAAMAAJ, 1994.

Tilman, D., Fargione, J., Wolff, B., D'Antonio, C., Dobson, A., Howarth, R., Schindler, D., Schlesinger, W. H., Simberloff, D. and Swackhamer, D.: Forecasting agriculturally driven global environmental change, Science (80-.)., 292(5515), 281–284, doi:10.1126/science.1057544, 2001.

Turkelboom, F., Poesen, J. and Trébuil, G.: The multiple land degradation effects caused by land-use intensification in tropical steeplands: A catchment study from northern Thailand, Catena, 75(1), 102–116, doi:10.1016/j.catena.2008.04.012, 2008.

Vogt, J. V., Safriel, U., Von Maltitz, G., Sokona, Y., Zougmore, R., Bastin, G. and Hill, J.: Monitoring and assessment of land degradation and desertification: Towards new conceptual and integrated approaches, L. Degrad. Dev., 22(2), 150–165, doi:10.1002/ldr.1075, 2011.

Wang, X., Huang, G. and Liu, J.: Projected increases in intensity and frequency of rainfall extremes through a regional climate modeling approach, JGR Atmos., 119(23), 13,271-286, doi:10.1038/175238c0, 2014.

Wheeler, T. and Von Braun, J.: Climate change impacts on global food security, Science (80-.)., 341(6145), 508–513, doi:10.1126/science.1239402, 2013.

Wildemeersch, J. C. J., Garba, M., Sabiou, M., Sleutel, S. and Cornelis, W.: The Effect of Water and Soil Conservation (WSC) on the Soil Chemical, Biological, and Physical Quality of a Plinthosol in Niger, L. Degrad. Dev., 26(7), 773–783, doi:10.1002/ldr.2416, 2015.

Williams, J. R.: The EPIC model, in Computer Models of Watershed Hydrology, edited by V. P. Singh, pp. 909–1000, Water Resources Publications., 1995.

Wirsenius, S.: Human Use of Land and Organic materials - Modeling the Turnover of Biomass in the Global Food System, Chalmers University of Technology and Göteborg University., 2000.

Wischmeier, W. H. and Smith, D. D.: Predicting rainfall erosion losses, Agric. Handb. no. 537, (537), 285–291, doi:10.1029/TR039i002p00285, 1978.

World Bank: World Bank Commodities Price Data (The Pink Sheet). available at: https://www.worldbank.org/en/research/commodity-markets (last access: 08.03.2021), [online] Available from: https://www.worldbank.org/en/research/commodity-markets, 2020a.

World Bank: World Development Indicators. available at: https://databank.worldbank.org/source/world-development-indicators (last access: 08.03.2021), [online] Available from: https://databank.worldbank.org/source/world-development-indicators, 2020b.

Wynants, M., Kelly, C., Mtei, K., Munishi, L., Patrick, A., Rabinovich, A., Nasseri, M., Gilvear, D., Roberts, N., Boeckx, P., Wilson, G., Blake, W. H. and Ndakidemi, P.: Drivers of increased soil erosion in East Africa's agro-pastoral systems: changing interactions between the social, economic and natural domains, Reg. Environ. Chang., 19(7), 1909–1921, doi:10.1007/s10113-019-01520-9, 2019.

Zhao, C., Liu, B., Piao, S., Wang, X., Lobell, D. B., Huang, Y., Huang, M., Yao, Y., Bassu, S., Ciais, P., Durand, J.-L., Elliott, J., Ewert, F., Janssens, I. A., Li, T., Lin, E., Liu, Q., Martre, P., Müller, C., Peng, S., Peñuelas, J., Ruane, A. C., Wallach, D., Wang, T., Wu, D., Liu, Z., Zhu, Y., Zhu, Z. and Asseng, S.: Temperature increase reduces global yields of major crops in four independent estimates, Proc. Natl. Acad. Sci., 201701762, doi:10.1073/pnas.1701762114, 2017.

Zheng, B., Campbell, J. B., Serbin, G. and Galbraith, J. M.: Remote sensing of crop residue and tillage practices: Present capabilities and future prospects, Soil Tillage Res., 138, 26–34, doi:10.1016/j.still.2013.12.009, 2014.
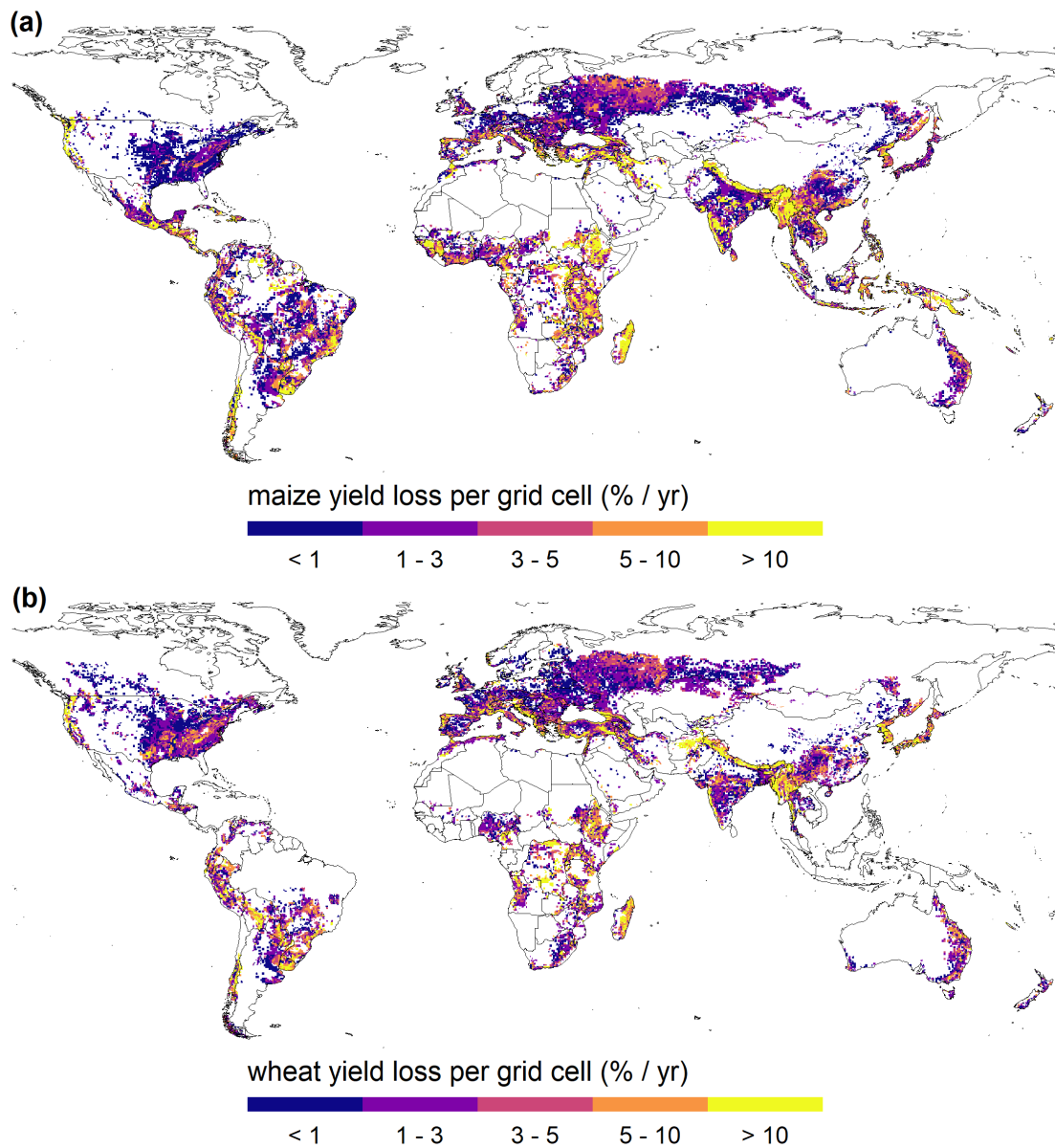
(a)

maize yield loss per grid cell (% / yr)

< 1   1 - 3   3 - 5   5 - 10   > 10

(b)

wheat yield loss per grid cell (% / yr)

< 1   1 - 3   3 - 5   5 - 10   > 10

Figure 1: Maize (a) and wheat (b) yield loss due to water erosion (% yr^{-1}) simulated with the baseline scenario and averaged for the years 2001 – 2010. Each grid cell is represented by one representative field capturing the most common site characteristics. Cropland areas are not considered in grid cell size.
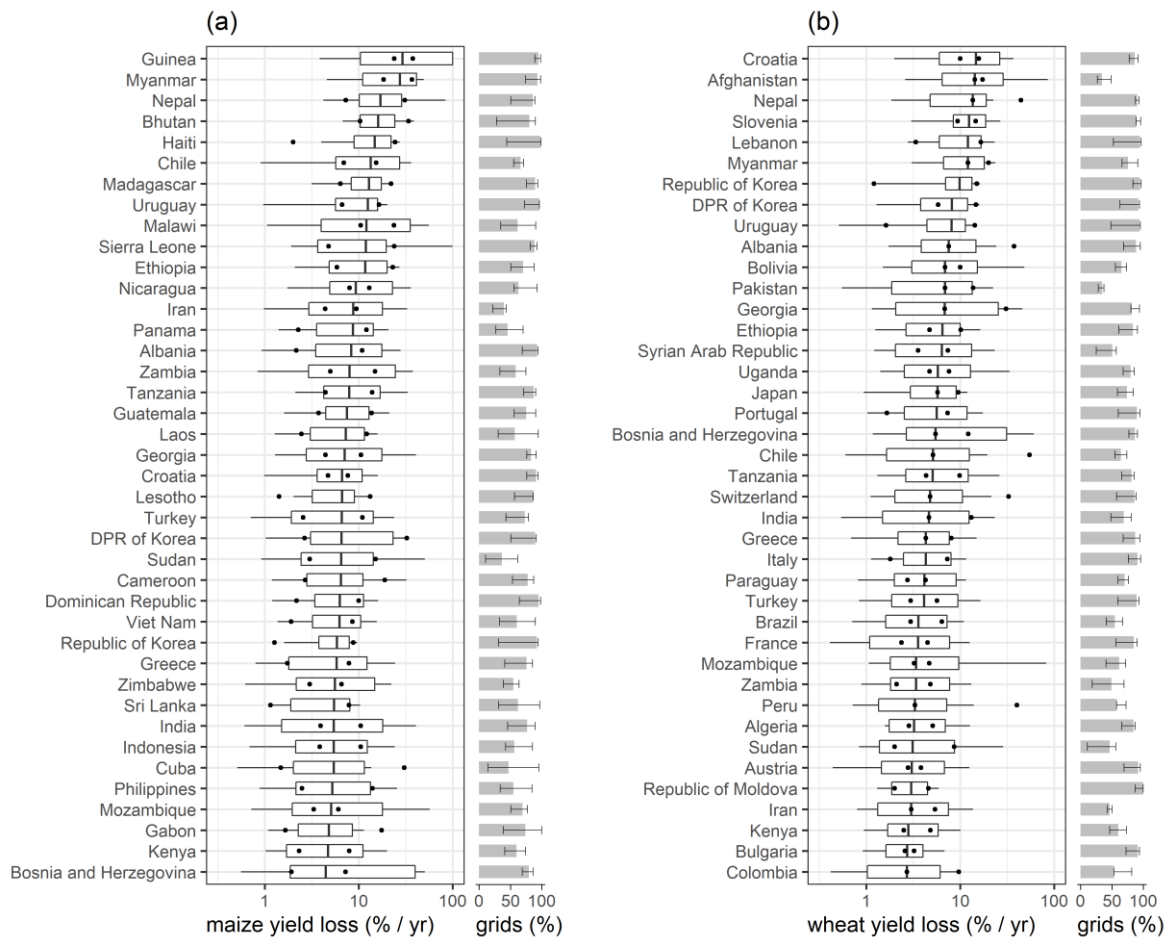
Figure 2: Maize (a) and wheat (b) yield losses due to water erosion (% yr⁻¹) for the 40 most vulnerable countries estimated with the baseline scenario. Countries contributing less than 0.01% to global maize and wheat production are excluded. The countries are ranked by median crop yield losses. Boxes include values from the 25th to the 75th percentiles and whiskers bracket values between the 10th and the 90th percentiles. The points illustrate minimum and maximum median crop yield losses generated from all field management scenarios. Medians and percentiles are converted to logarithmic scale. Grey barplots on the right illustrate the share of grid cells affected by water erosion impacts in each country, and errorbars indicate the variability of affected grid cells due to all management scenarios. The distributions of all relevant maize and wheat producing countries are provided in Figure S8 and Figure S9.
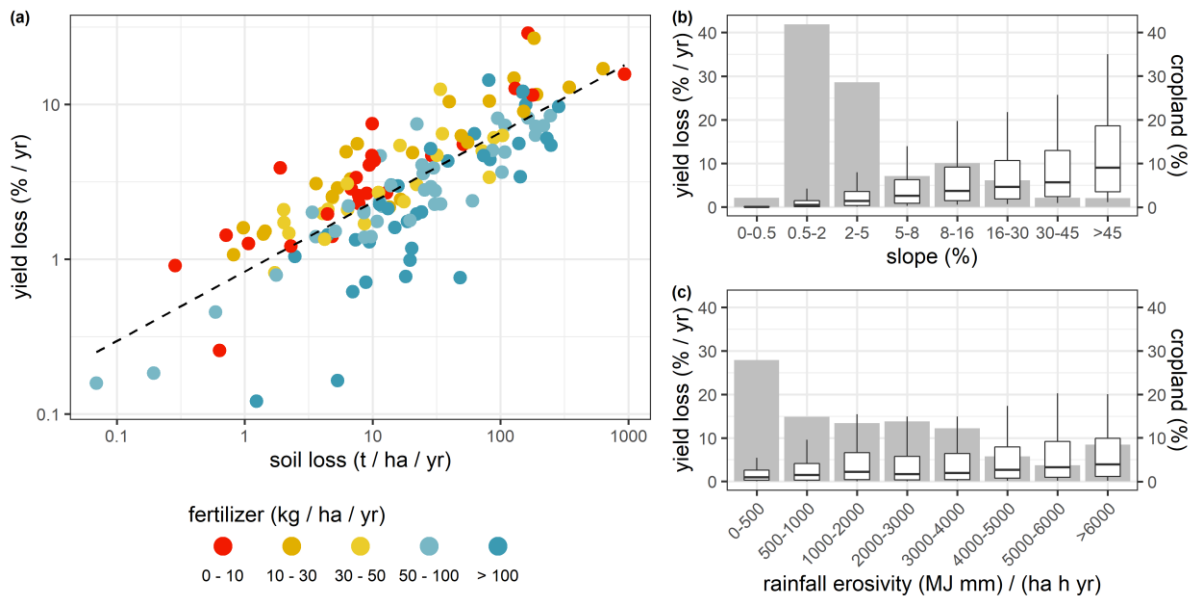
Figure 3: (a) Modelled median maize and wheat yield loss plotted against median soil loss through water erosion for each country. The linear relationship between national soil loss and crop yield loss is illustrated by the dashed regression line. Colours indicate the rate of fertilizer application per country. (b,c) Maize and wheat yield losses, respectively, per grid cells classified by slope steepness and rainfall erosivity. Grey bars illustrate the share of cropland in grid cells summarised for the different slope and rainfall erosivity classes.
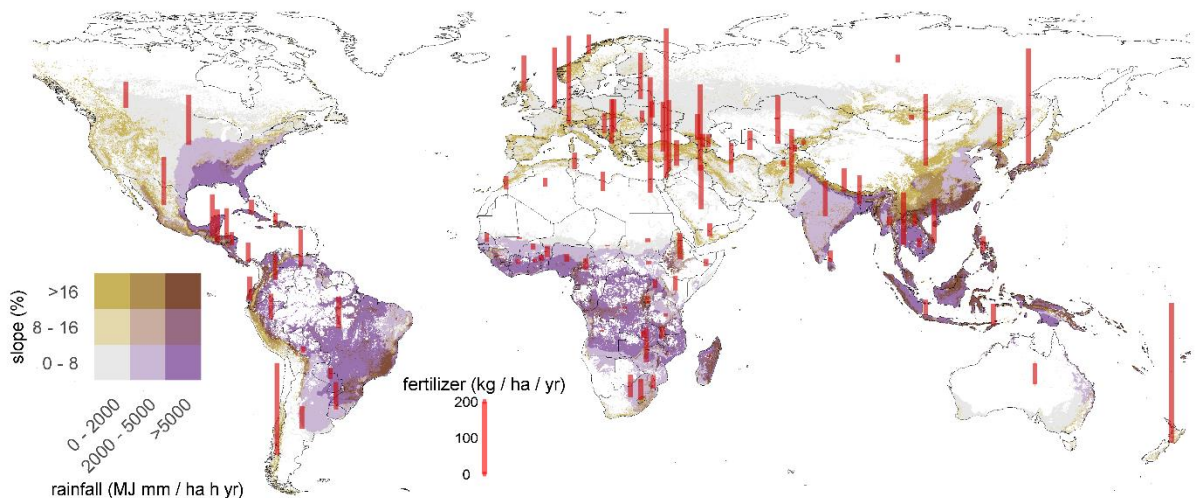

Figure 4: water erosion vulnerability on global cropland indicated through the most important environmental drivers, rainfall erosivity (MJ mm ha^{-1} h^{-1} yr^{-1}) and slope steepness (%), and the average sum of Nitrogen, Phosphorous and Potassium fertilizer application rates (kg ha^{-1}yr^{-1}) per country represented by the red bars. To improve the
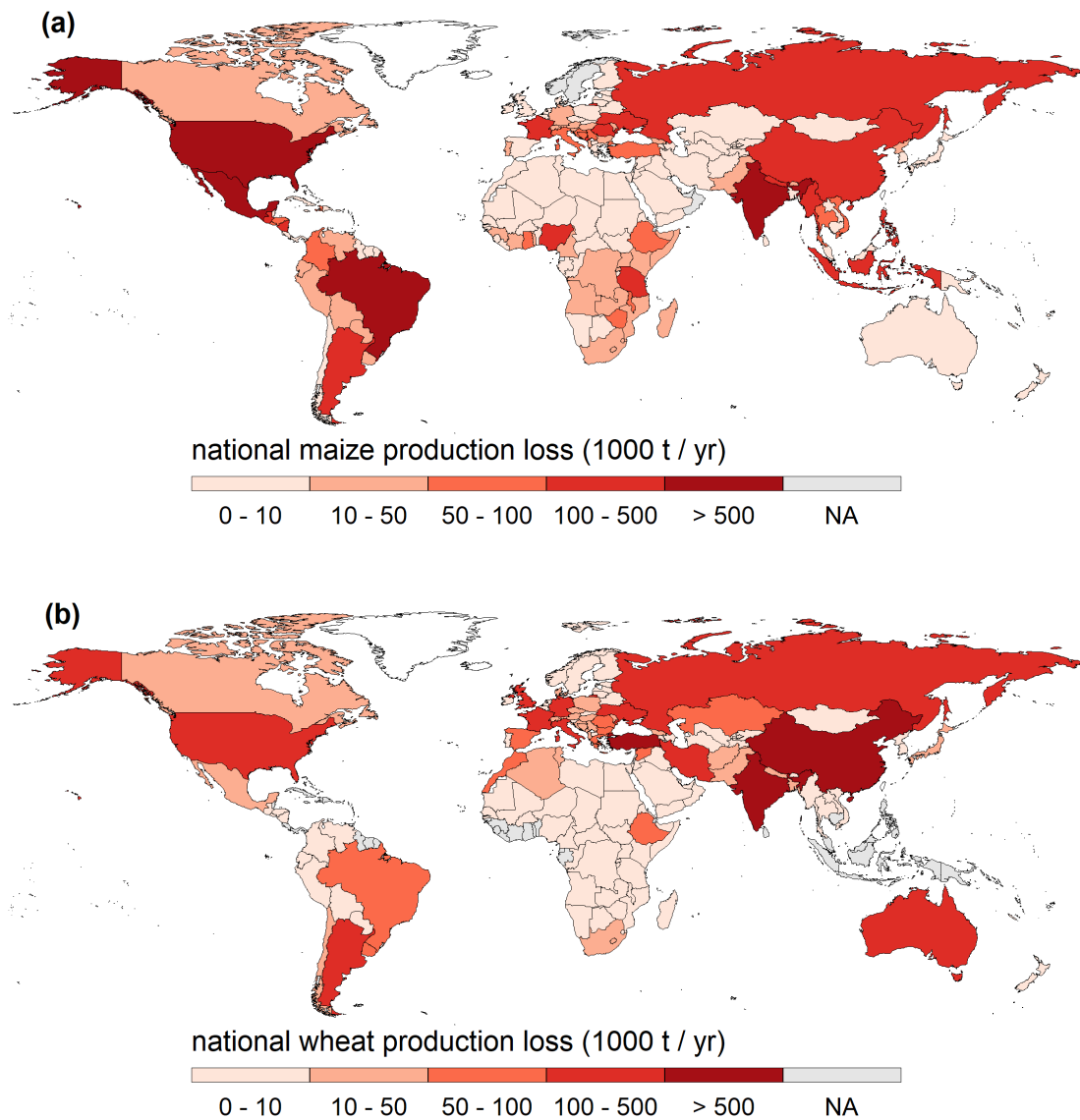
Figure 5: The impact of water erosion on national maize (a) and wheat (b) production based on the sum of estimated production losses in all grid cells in each country. NA marks countries without maize or wheat production area. Estimates of production losses in each grid cell assume uniform site characteristics for the entire cropland in each grid cell.
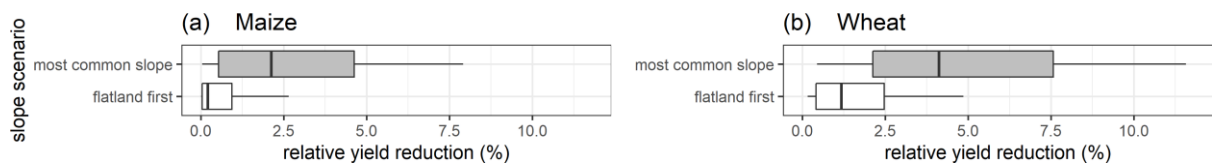
Figure 6: Range of simulated maize and wheat yield losses (% yr⁻¹) in Italy simulated with different cropland distribution scenarios for maize (a) and wheat (b). Boxes illustrate medians and 25th and 75th percentiles, whiskers illustrate values between the 10th and the 90th percentiles. Grey bars mark the baseline scenario used for the main results of this study.

Table 1: input settings for the conventional, reduced and no-tillage scenario

	Conventional tillage	Reduced tillage	No-tillage
total cultivation operations	6–7	4–5	3
max. tillage depth	150 mm	150 mm	40–60 mm
mixing efficiency	99%	75%	2%
max. surface roughness	30–50 mm	20 mm	10 mm
plant residues left	25%	50%	75%
cover treatment class	straight	contoured	contoured & terraced

Table 2: Countries with the highest annual maize production losses. All records are provided in Table S2.

country	prod. (million t)[+]	prod. loss (million t)[*]	prod. loss (%)	prod. loss (million $)[+]
Mexico	25.6	1.3	5.0	264.8
Brazil	81.6	0.8	1.0	157.7
USA	376.7	0.7	0.2	104.9
India	25.6	0.6	2.5	92.0
China	246.7	0.5	0.2	199.8
Indonesia	23.3	0.5	2.1	151.8
Philippines	7.6	0.4	5.2	111.3
Nepal	2.2	0.3	12.5	74.2
Guatemala	1.9	0.2	12.8	37.2
Russia	12.7	0.2	1.5	24.6

country	prod. (million t)[+]	prod. loss (million t)[*]	prod. loss (%)	prod. loss (million $)[+]
Argentina	38.6	0.2	0.5	31.1
Tanzania	6.0	0.2	2.7	29.8
Nigeria	10.2	0.1	1.3	41.2
Myanmar	1.8	0.1	6.5	27.1
Nicaragua	0.4	0.1	27.8	31.9
Romania	12.7	0.1	0.9	20.6
Ukraine	28.6	0.1	0.4	14.8
France	14.4	0.1	0.7	17.9
Ethiopia	7.5	0.1	1.3	20.8
Viet Nam	5.2	0.1	1.7	26.4
World	1,091.1	8.9	0.8	1,960.7

+*FAOSTAT: 2013 - 2018 or the latest five years recorded.*

assuming uniform cropland in each grid cell.

Table 3: Countries with the highest annual wheat production losses. All records are provided in Table S3.

country	prod. (million t)[+]	prod. loss (million t)*	prod. loss (%)	prod. loss (million $)[+]
India	94.4	0.7	0.7	137.4
China	130.0	0.6	0.5	213.7
Turkey	21.0	0.5	2.5	139.4
USA	55.1	0.5	0.8	89.4
Russia	67.5	0.4	0.6	60.2
France	37.4	0.3	0.8	56.9
Argentina	13.2	0.2	1.8	56.5
Iran	12.4	0.2	1.6	77.4
United Kingdom	14.6	0.1	1.0	30.1
Italy	7.3	0.1	1.9	32.5
Germany	24.8	0.1	0.5	22.9
Ukraine	25.0	0.1	0.5	17.7

country	prod. (million t)[+]	prod. loss (million t)*	prod. loss (%)	prod. loss (million $)[+]
Australia	24.5	0.1	0.4	22.0
Kazakhstan	14.1	0.1	0.6	11.3
Spain	6.9	0.1	1.2	17.9
Syria	2.0	0.1	3.6	9.7
Morocco	6.2	0.1	1.1	19.4
Romania	8.6	0.1	0.8	11.9
Greece	1.5	0.1	4.4	15.8
Ethiopia	4.4	0.1	1.4	23.4
World	739.5	5.6	0.8	1,292.5

+*FAOSTAT: 2013 - 2018 or the latest five years recorded.*

* assuming uniform cropland in each grid cell.